Seismic Evidence for Olivine Phase Changes at the 410- and 660-Kilometer Discontinuities

Sergei Lebedev, Sebastien Chevrot,

Rob D. van der Hilst

Overview

- Some disagreement about what phase change(s) cause the 660
  - Irifune et al (1998), e.g.: suggest post-spinel occurs at 22 GPa, as opposed to 24 GPa
  - Seismic results ambiguous
  - Gt-Pv and Gt-Il-Pv suggested
- This paper uses estimates of Vs from tomography studies and differential travel times from incoming Pds waves to calculate the seismic Clapeyron slope and thus constrain the phase changes that could be responsible for the 660.

Seismically Inferred Clapeyron Slope

- It is not meaningful to define thermodynamic Clapeyron slopes for the 410 and 660, since there are multiple phases
- Bina & Helffrich (1994) define the seismic Clapeyron slope, which can be determined experimentally and is dependent on thermodynamic properties.
- Seismic Clapeyron slope can be affected by isostructural phases with variable chemistry at the depth of the discontinuity, in particular because of the exchange of Mg and Fe between olivine and other minerals.

Correlation between TZ thickness and TZ temperature.

- If the 660 is caused by the post-spinel phase change, then the 410 and 660 should be deflected away (towards) each other for a cold (hot) anomaly.
- The height of the TZ (HTZ) would then correlate with TZ temperature, as well as with Vs within the TZ (since Vs is temperature dependent).
- If the 660 is caused by the gt-pv transition, which has a positive Clapeyron slope, the correlation between HTZ and temperature (and HTZ and Vs) would be weak or absent.

P410s and P660s have the same ray paths, to first order, so any time differences should be due to structure in the transition zone (TZ), where P660s is an S-wave and P410s is a P wave.

Image removed due to copyright considerations.

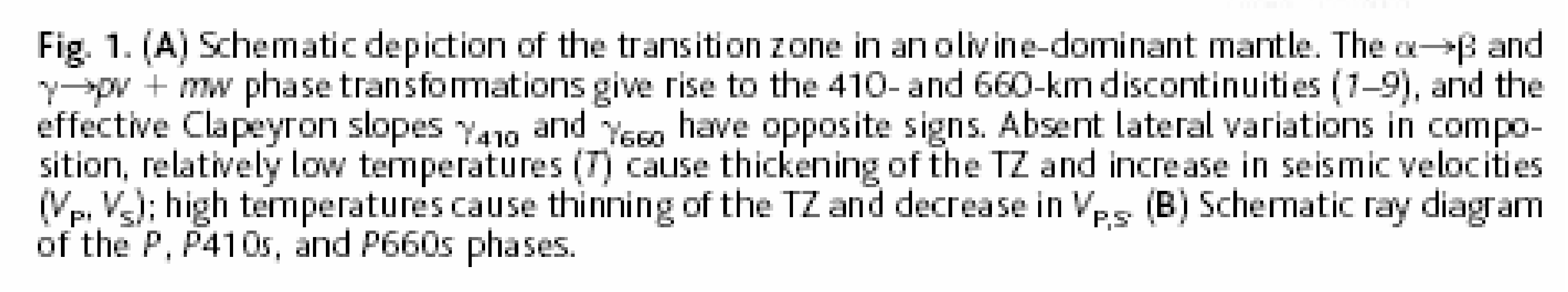

Fig. 1. **(A)** Schematic depiction of the transition zone in an olivine-dominant mantle. The $\alpha \rightarrow \beta$ and $\gamma \rightarrow pv + mw$ phase transformations give rise to the 410- and 660-km discontinuities (*1–9*), and the effective Clapeyron slopes γ_{410} and γ_{660} have opposite signs. Absent lateral variations in composition, relatively low temperatures (T) cause thickening of the TZ and increase in seismic velocities (V_P, V_S); high temperatures cause thinning of the TZ and decrease in $V_{P,S}$. **(B)** Schematic ray diagram of the *P*, *P*410*s*, and *P*660*s* phases.

Initial stations used

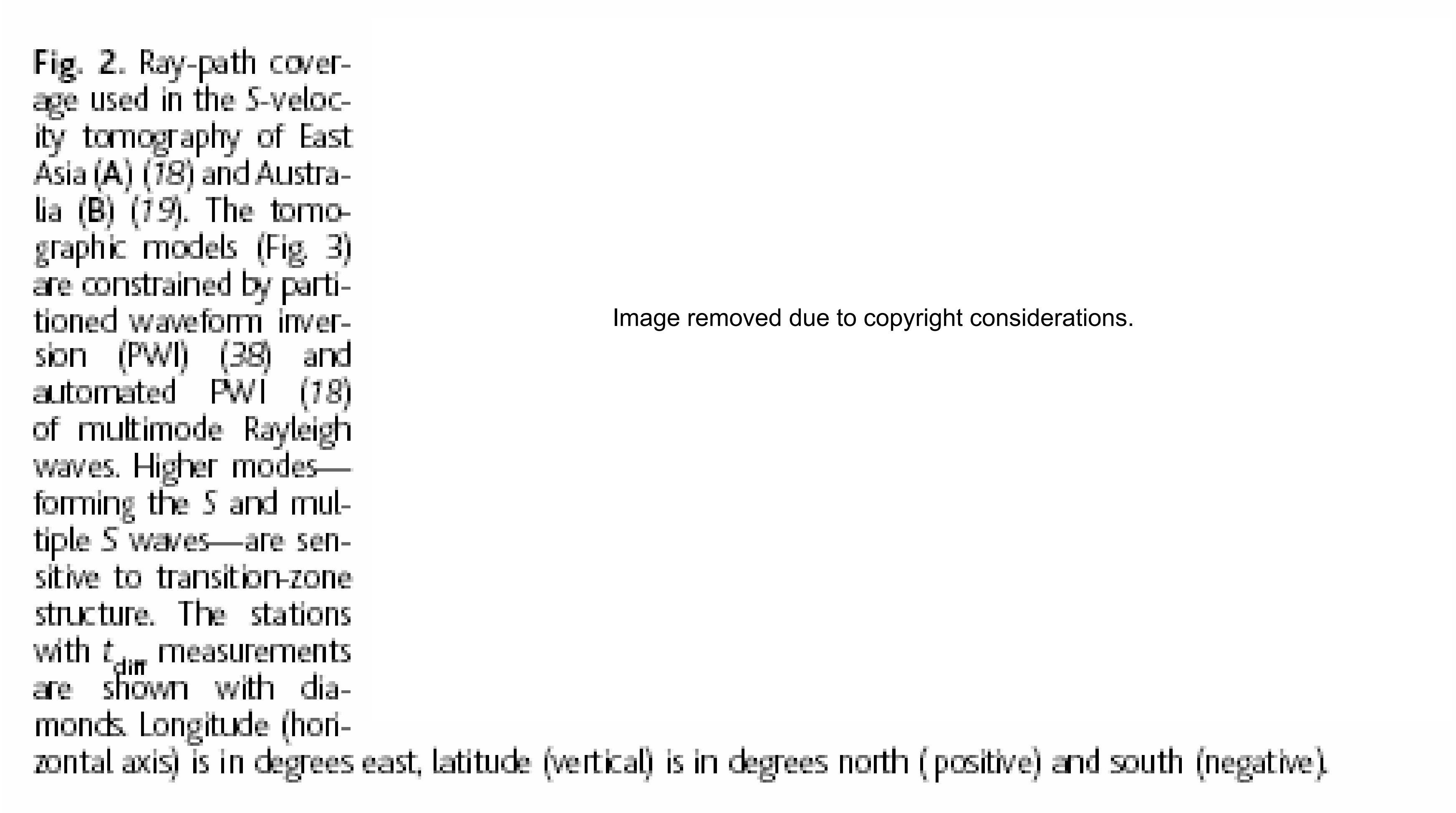

Fig. 2. Ray-path coverage used in the S-velocity tomography of East Asia (**A**) (*18*) and Australia (**B**) (*19*). The tomographic models (Fig. 3) are constrained by partitioned waveform inversion (PWI) (*38*) and automated PWI (*18*) of multimode Rayleigh waves. Higher modes—forming the *S* and multiple *S* waves—are sensitive to transition-zone structure. The stations with t_{diff} measurements are shown with diamonds. Longitude (horizontal axis) is in degrees east, latitude (vertical) is in degrees north (positive) and south (negative).

Image removed due to copyright considerations.

Data selection

- Pds waves used to calculate tdiff:

  t(diff) = t(P660s) – t(P410s)

- Reject traces with low signal-to-noise ratios, stacks that didn’t show both P660s and P410s, and stations which did not have enough acceptable traces.
- Used previously determined tomographic model values of Vs at their stations.
- Reliable estimates for the upper (δVs_{410}) and lower (δVs_{660}) parts of the TZ obtained for eight stations.

Stations used

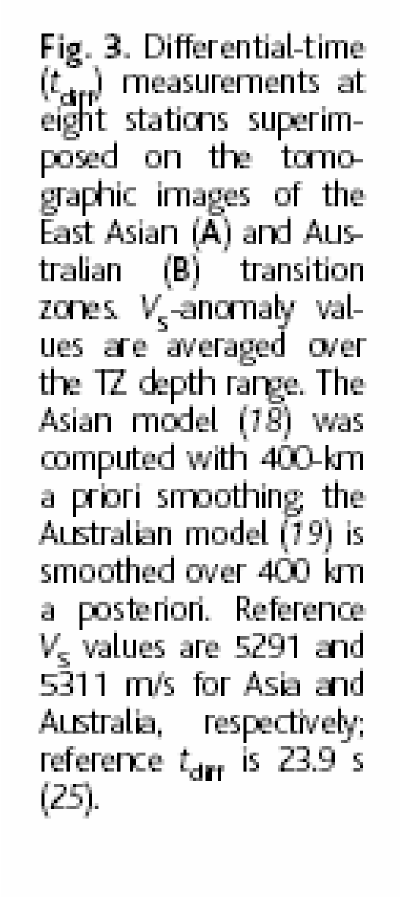

Fig. 3. Differential-time (t_{diff}) measurements at eight stations superimposed on the tomographic images of the East Asian (**A**) and Australian (**B**) transition zones. V_S-anomaly values are averaged over the TZ depth range. The Asian model (*18*) was computed with 400-km a priori smoothing; the Australian model (*19*) is smoothed over 400 km a posteriori. Reference V_S values are 5291 and 5311 m/s for Asia and Australia, respectively; reference t_{diff} is 23.9 s (*25*).

Image removed due to copyright considerations.

Results I

- tdiff correlates with $\delta Vs_{TZ} = \delta Vs_{410} + \delta Vs_{660}$ (r = .94)
- For a TZ of constant thickness, tdiff would have negative correlation with velocity.
- Convert tdiff to HTZ anomaly (δHTZ) using P and S velocities from iasp91, δVs_{TZ}, and $R = \delta \ln Vs/\delta \ln Vp = 1.7$ +/- 0.7
- Convert δVs_{TZ} to δT_{TZ} (temperature anomaly) using $\partial \ln Vs/\partial T = -1.35 \times 10^{-4} K^{-1}$ and a $0.4 \times 10^{-4} K^{-1}$ uncertainty.
- HTZ correlates with δT_{TZ} with r = 0.98; slope of best fitting line = -0.13 =/- 0.07 km/K; consistent with slope inferred from mineralogical Clapeyron slopes of alpha-beta and post-spinel phase changes.

Fig. 4. The correlation between (A) S velocity in the transition zone and the differential time t_{diff} and between (B) the inferred temperature of the transition zone T_{TZ} and its thickness H_{TZ}. Seismic velocity anomalies δV_S^{TZ} are vertical averages over the transition-zone depth range, and so are the estimated temperature anomalies δT_{TZ}. The data from the East Asian stations are shown with dark-shaded symbols (BJT, with a square; ENH, triangle; QIZ, inverted triangle; SSE, diamond; XAN, circle). The data from the Australian stations are shown with light-shaded symbols (CTAO, with a square; SA03, inverted triangle; STKA, triangle).

Image removed due to copyright considerations.

Results II: Clapeyron slope

- Use δVs estimates to compute seismic Clapeyron slopes (γ_{410} and γ_{660})

$$\delta HTZ = (\partial d/\partial P)_{660} \times \gamma_{660} \times (\partial T/\partial \ln Vs)\delta \ln Vs_{660} - (\partial d/\partial P)_{410} \times \gamma_{410} \times (\partial T/\partial \ln Vs)\delta \ln Vs_{410}$$

$(\partial d/\partial P)_{660(410)}$ describes the depth-pressure relationship at the 660(410)

- Find γ_{410} and γ_{660} by minimizing chi-square function $\delta HTZ_i - \delta HTZ$, δHTZ_i the data at the ith station and δHTZ calculated

Small square is mineralogical Clapeyron slope from Bina & Helffrich (1994); large rectangle is range of values as compiled by Bina & Helffrich (1994)

Image removed due to copyright considerations.

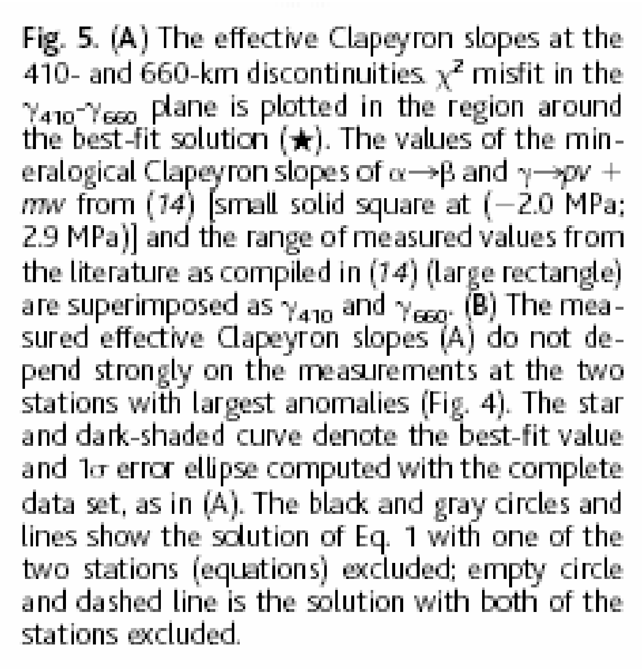

Fig. 5. (**A**) The effective Clapeyron slopes at the 410- and 660-km discontinuities. χ^2 misfit in the γ_{410}-γ_{660} plane is plotted in the region around the best-fit solution (★). The values of the mineralogical Clapeyron slopes of $\alpha \rightarrow \beta$ and $\gamma \rightarrow pv + mw$ from (*14*) [small solid square at (−2.0 MPa; 2.9 MPa)] and the range of measured values from the literature as compiled in (*14*) (large rectangle) are superimposed as γ_{410} and γ_{660}. (**B**) The measured effective Clapeyron slopes (A) do not depend strongly on the measurements at the two stations with largest anomalies (Fig. 4). The star and dark-shaded curve denote the best-fit value and 1σ error ellipse computed with the complete data set, as in (A). The black and gray circles and lines show the solution of Eq. 1 with one of the two stations (equations) excluded; empty circle and dashed line is the solution with both of the stations excluded.

Conclusions

- The seismic Clapeyron slopes found for the 410 and 660 are consistent with the mineralogical Clapeyron slopes of the olivine transformations
- Inconsistencies with other studies, where weak correlations between tdiff and Vs_{TZ} have been found, is due to differences in spatial resolution between tdiff and Vp_{TZ} and Vs_{TZ} from global tomography.